

Lifetime Estimates with Single-Multilayer Breakup Probability Differences

Daniel Goldin
University of Basel

May 27, 2005

Abstract

In this note we describe the method of finding ponium atom $1s$ state lifetime for the 2002 24 GeV and 2003 20 GeV runs by considering single - multilayer target breakup probability *differences*. While the method of the single/multilayer breakup probability *ratios* [1] avoids the systematics associated with the normalization, we show that there are reasons to believe that the method of probability differences, discussed here, results in smaller *overall* systematic error, as shown below. We employ the standard and modified (Basel) track reconstructions in this study.

The Method of Breakup Probability Differences

We begin by normalizing Q_l and Q *multiayer distributions to the single layer ones*. (The inverse normalization is, of course, also possible and will, in fact, be used later.) Subtracting single from multilayer distributions yields the spectra similar to the ones shown in Fig. 1. The residuals, which we denote by δ , are found by summing the bins in the signal area ($Q_l < 2$ MeV/ c , $Q < 4$ MeV/ c). The results, along with the associated statistical error, for the standard and modified (Basel) tracking are shown in Table 1.

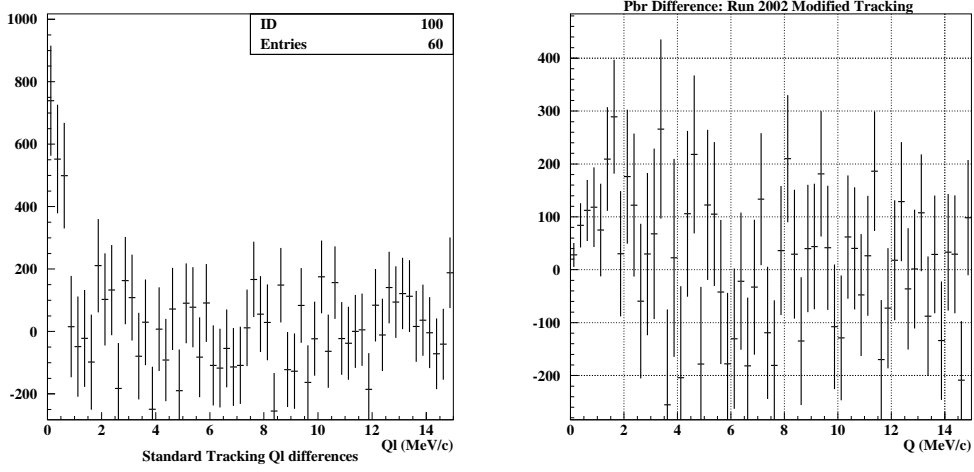


Fig. 1: Run 2002 (24 GeV) Q_l and Q single - multilayer differences.

Tracking	2002		2003	
	$\delta(Q_l)$	$\delta(Q)$	$\delta(Q_l)$	$\delta(Q)$
Standard	1849 ± 453	1912 ± 514	521 ± 208	547 ± 235
Modified	1504 ± 438	1315 ± 499	365 ± 201	546 ± 227

Table 1: Signal differentials (residuals) found by subtracting multi- from single layer Q_l and Q distributions (multilayer-to-single layer normalization). The residuals are calculated by integrating the signal in the $Q_l < 2$ MeV/c, $Q < 4$ MeV/c intervals.

Next, we consider the Monte Carlo-simulated background. For this purpose, atomic (AT), Coulomb (CC), non-Coulomb (NC) and accidental (ACC) events were generated and processed by GEANT-DIRAC [2].¹ *The MC background obtained with 2002 detector configuration and the single layer 98 μm target were used throughout this study to analyze the single and multilayer data for both 2002 and 2003 runs.*² Tracks were reconstructed by ARIANE [3], Version 304.31.

Using the initial and reconstructed Q_l and Q distributions for atomic and Coulomb pairs we calculate the effective K -factor through:

$$K_{eff}(Q_l) = K_{th} \frac{n_A(Q_l < Q_l^{cut})}{n_A} \frac{N_{cc}(Q^{init} < 2 \text{ MeV}/c)}{N_{cc}(Q_l < Q_l^{cut})} \quad (1)$$

and

$$K_{eff}(Q) = K_{th} \frac{n_A(Q < Q^{cut})}{n_A} \frac{N_{cc}(Q^{init} < 2 \text{ MeV}/c)}{N_{cc}(Q < Q^{cut})}. \quad (2)$$

With cuts set at $Q_l^{cut} < 2 \text{ MeV}/c$, $Q^{cut} < 4 \text{ MeV}/c$, we obtain the following values of the K_{eff} (Table 2).

Tracking	$K_{eff}(Q_l)$	$K_{eff}(Q)$
Standard	0.1713 ± 0.0007	0.1341 ± 0.0005
Modified	0.1748 ± 0.0005	0.1355 ± 0.0004

Table 2: Effective K -factor values computed from 2002 24 GeV atomic and Coulomb Q_l and Q distributions. These values were also used to analyze the 2003 20 GeV data.

Next, we perform the background fit in one parameter ω , which expresses the fraction of Coulomb pairs in the combined Coulomb + non-Coulomb pair sample. The following parametrization was used:

$$\frac{dN_B}{dQ_l} = \beta \left[(1 - \phi_{acc}) \left[\omega \frac{dN_{cc}}{dQ_l} + (1 - \omega) \frac{dN_{nc}}{dQ_l} \right] + \phi_{acc} \frac{dN_{acc}}{dQ_l} \right]. \quad (3)$$

¹Input files were provided by C. Santamarina.

²The equivalence of the single and multilayer backgrounds were demonstrated in Ref. [1]. However, using the 2002 24 GeV data to study 2003 20 GeV results, as we do here, leads to slight loss of accuracy, as also discussed in Ref. [1].

The fit was performed simultaneously in Q_l and Q .³ Here ϕ expresses the fraction of accidentals in the background events. The values of ϕ were found to vary between 8.2% to 9.3% depending on the run year and the type of tracking. The exact value of the accidental contribution is of little importance to the overall systematics [1]. Factor β determines the overall normalization of the background. (With β absent, the background in Eq. 3 would be normalized to 1.) β is found by integrating the experimental background in the given fit interval. For this study a set of intervals between 2 and 15 MeV/ c in Q_l and 4 and 15 MeV/ c in Q in steps of 0.25 MeV/ c were used. Sample values of the fit parameter ω for the $2 \text{ MeV}/c \leq Q_l \leq 15 \text{ MeV}/c$ and $4 \text{ MeV}/c \leq Q \leq 15 \text{ MeV}/c$ fits are shown in Table 3.

Tracking	2002		2003	
	$\omega(Q_l)$	$\omega(Q)$	$\omega(Q_l)$	$\omega(Q)$
Standard	0.9123 ± 0.0109	0.9058 ± 0.0196	0.8950 ± 0.0175	0.9186 ± 0.0313
Modified	0.8801 ± 0.0105	0.9016 ± 0.0196	0.9084 ± 0.0180	0.9171 ± 0.0330

Table 3: Sample values of the fit parameter ω shown for 2 to 15 MeV/ c fit in Q_l and 4 to 15 MeV/ c fits in Q . The values of ω do not vary appreciably for other fit ranges.

	2002		2003	
	Q_l	Q	Q_l	Q
Standard Tracking				
$\delta_{Q_l, Q}$	1849 ± 453	1912 ± 514	521 ± 208	547 ± 235
$N_{cc(Q_l, Q < Q_{cut})}$	56092 ± 2945	72508 ± 3286	18190 ± 1205	21952 ± 1290
ΔP_{br}	0.1922 ± 0.0481	0.1963 ± 0.0536	0.1678 ± 0.0679	0.1737 ± 0.0754
Modified Tracking				
$\delta_{Q_l, Q}$	1504 ± 438	1315 ± 499	365 ± 201	546 ± 227
$N_{cc(Q_l, Q < Q_{cut})}$	52558 ± 2806	69181 ± 3130	16831 ± 1153	21952 ± 1290
ΔP_{br}	0.1635 ± 0.0484	0.1401 ± 0.0537	0.1278 ± 0.0707	0.1875 ± 0.0787

Table 4: Differentials from Table 1, the integral number of Coulomb pairs corresponding to Eq. 5 and the resulting values of ΔP_{br} for Q_l and Q averaged over 8 to 15 MeV/ c intervals.

³The equations that follow from this point on are expressed in terms of Q_l . Their counterparts in Q are completely analogous, except for the signal cutoff point at $Q < 4$ MeV/ c , in place of $Q_l < 2$ MeV/ c .

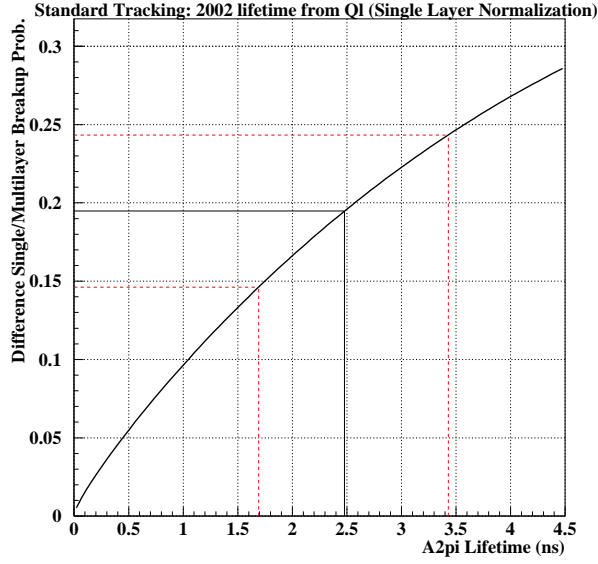


Fig. 2: Breakup probability difference vs. lifetime parametrization. Breakup and lifetime with corresponding errors for 2002 run with standard tracking in Q_l are shown.

	2002		2003	
Tracking	$\tau(Q_l)$	$\tau(Q)$	$\tau(Q_l)$	$\tau(Q)$
Standard	$2.43^{+0.93}_{-0.77}$	$2.51^{+1.06}_{-0.87}$	$2.02^{+1.24}_{-0.98}$	$2.12^{+1.44}_{-1.10}$
Modified	$1.96^{+0.83}_{-0.71}$	$1.60^{+0.86}_{-0.73}$	$1.42^{+1.12}_{-0.90}$	$2.35^{+1.61}_{-1.19}$

Table 5: Pionium lifetimes as a function of Q_l and Q obtained with the breakup probability difference method. The values correspond to the breakup probability differences averaged over 8 to 15 MeV/c intervals.

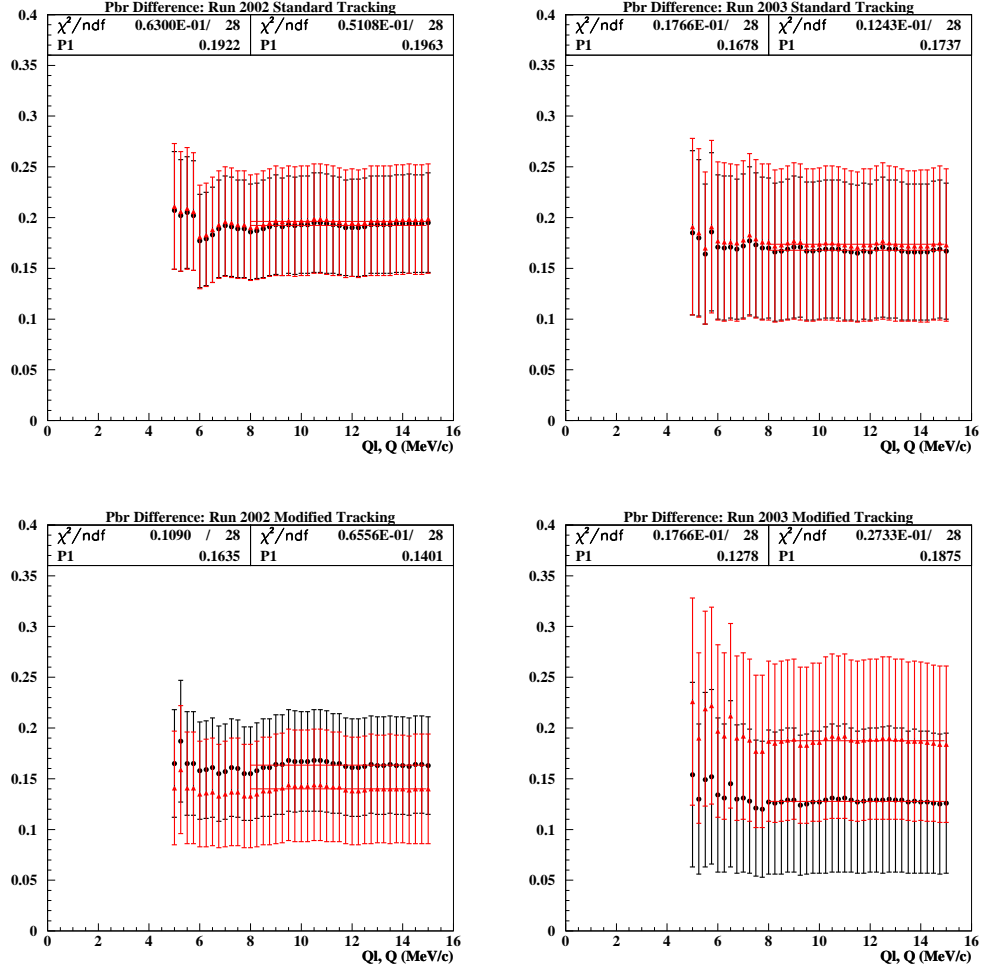


Fig. 3: Single - multilayer breakup probability differences in Q_l and Q plotted together. Final values of ΔP_{br} in Q_l and Q were selected based on the zero-slope straight line fit (filled circles correspond to Q_l fits, upturned triangles to Q fits).

We now have all the ingredients available to calculate the single-multilayer breakup probability differences, ΔP_{br} .

$$\begin{aligned}\Delta P_{br} &= \frac{n_A^S}{K_{eff}N_{cc}(Q_l < 2)} - \frac{n_A^M}{K_{eff}N_{cc}(Q_l < 2)} \\ &= \frac{n_A^S - n_A^M}{K_{eff}N_{cc}(Q_l < 2)} = \frac{\delta_{Q_l}}{K_{eff}N_{cc}(Q_l < 2)},\end{aligned}\quad (4)$$

where n_A^S and n_A^M are the single and multilayer residuals, respectively. N_{cc} here refers to the integral of the Coulomb contribution to the overall background fit, e.g. for Q_l from Eq. 3:⁴

$$N_{cc}(Q_l < 2) = \int_0^2 \beta(1 - \phi_{acc})\omega \frac{dN_{cc}}{dQ_l} dQ_l \quad (5)$$

ΔP_{br} vs. lifetime curve is found by subtracting the P_{br} vs. lifetime parametrization for the single layer and subtracting its analog for the multilayer target [4]. The result is shown in Fig. 2.

ΔP_{br} for various fit ranges is shown in Fig. 3. For each run period/tracking method only one value of ΔP_{br} in Q_l or Q was taken by fitting zero-slope straight line to the plots in the range from 8 to 15 MeV/c. In Table 4 we summarize the essential ingredients of Eq. 4 The corresponding values of τ_{1s} are shown in Table 5.

Breakup Probability Ratios vs. Lifetime

In this section we examine the method of taking the *ratios* of the breakup probabilities. This method is qualitatively different from the previous one in that the use of K -factor can be avoided here. Since in the previous section we have used the residual signal in the analysis, for the sake of consistency we also apply this method here (Ref. [1] uses the atomic shape fit instead.)

The ratio of breakup probabilities (assuming single-to-multilayer or multi-to-single layer normalization) can be expressed as:

$$\rho \equiv \frac{P_{br}^s}{P_{br}^m} = \frac{\sum_i N_{at}^s(Q_i)}{\sum_i N_{at}^m(Q_i)}, \quad (6)$$

⁴We remind the reader that the individual values of n_A^S and n_A^M depend on which normalization was chosen (single-to-multilayer or multi-to-single layer), as does the value of $N_{cc}(Q_l < 2)$.

where $\sum_i N_{at}^s(Q_i)$ and $\sum_i N_{at}^m(Q_i)$ are the atomic pair signals in the single layer and multilayer targets respectively. One can improve the statistical accuracy of this ratio by considering the sum and the difference of the atomic pair signals. Then if

$$\sigma \equiv \sum_i N_{at}^s(Q_i) + \sum_i N_{at}^m(Q_i) \quad (7)$$

$$\delta \equiv \sum_i N_{at}^s(Q_i) - \sum_i N_{at}^m(Q_i) \quad (8)$$

then ρ can be found through:

$$\rho = \frac{\sigma + \delta}{\sigma - \delta} \quad (9)$$

For this study we *normalize the single layer data to the multilayer ones*. A background fit to the *sum* of the single and multilayer Q_l and Q distributions is made using fit parameter ω , which has the same physical meaning as in the previous section. The signal (σ) is found by subtracting the experimental data from the background fits. As before, the residual signal was calculated in the $Q_l < 2$ and $Q < 4$ MeV/ c intervals. The results for various fit regions are plotted in Fig. 4.

In Fig. 4 significant variations of the signal strengths depending on the fit range is observed, and all four plots exhibit large Q_l - Q differences in σ .

δ is found in the same way as discussed in the beginning of the previous section, with the exception of the *single-to-multilayer* normalization. The results are shown in Table 6.⁵

	2002		2003	
Tracking	$\delta(Q_l)$	$\delta(Q)$	$\delta(Q_l)$	$\delta(Q)$
Standard	846 ± 207	873 ± 235	490 ± 196	515 ± 221
Modified	704 ± 205	615 ± 233	345 ± 190	516 ± 215

Table 6: Signal differentials (residuals) found by subtracting single from multilayer Q_l and Q distributions (*multilayer normalization*). The residuals are calculated by integrating the signal in the $Q_l < 2$ MeV/ c , $Q < 4$ MeV/ c intervals.

Using Eq. 9 and the results of Fig. 4 and Table 6, we obtain the fit-range dependent ρ distributions for Q_l and Q (Fig. 5).

⁵The values of this table represent the correction of the several erroneous values found in the bottom Table 8.2 in Ref. [1].

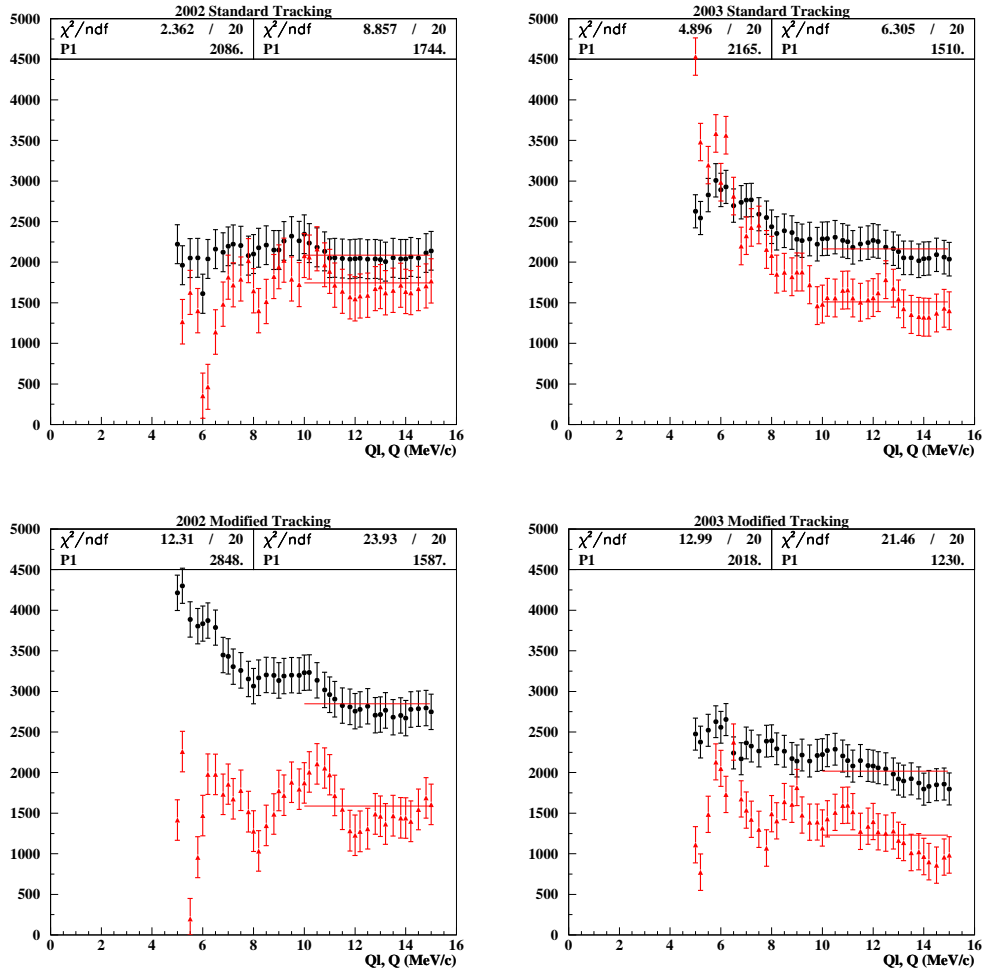


Fig. 4: Values of the signal (σ) for Q_l and Q (plotted together) as a function of the fit range for the two tracking methods and run periods filled circles correspond to Q_l fits, upturned triangles to Q fits).

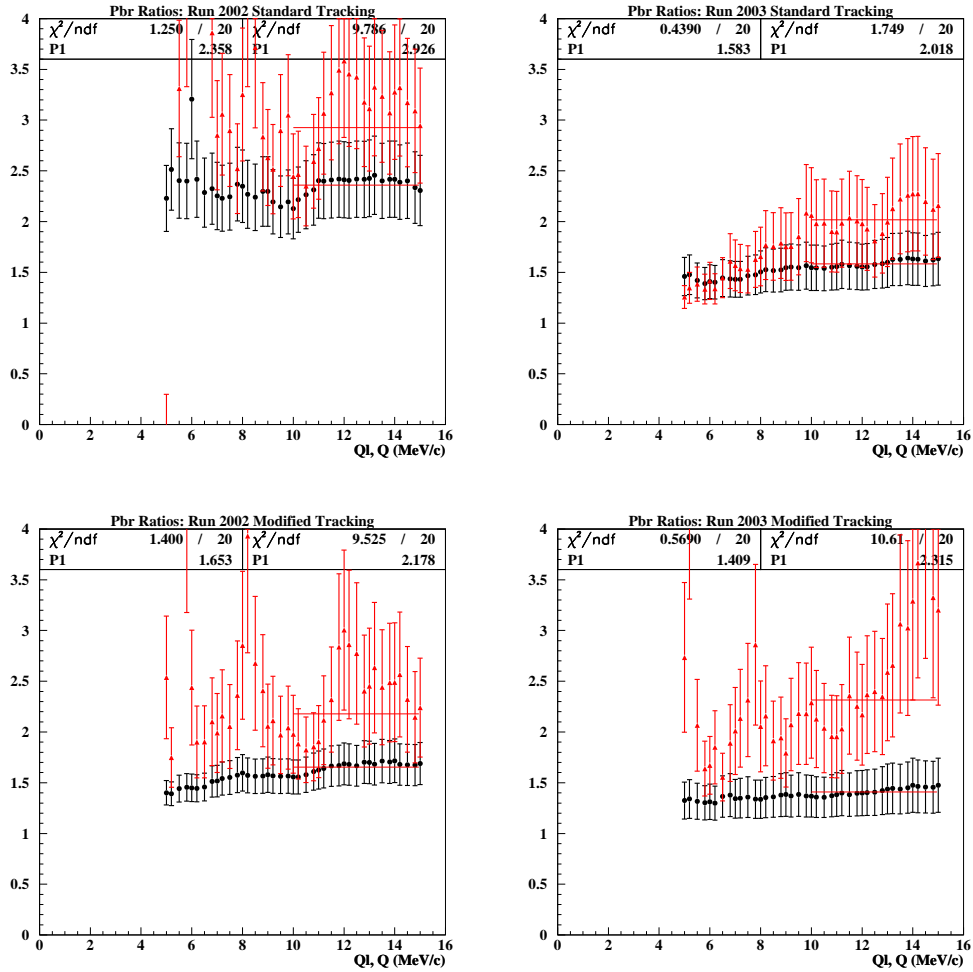


Fig. 5: Values of the breakup probability ratios (ρ) for Q_l and Q (plotted together) as a function of the fit range for the two tracking methods and run periods (filled circles correspond to Q_l fits, upturned triangles to Q fits).

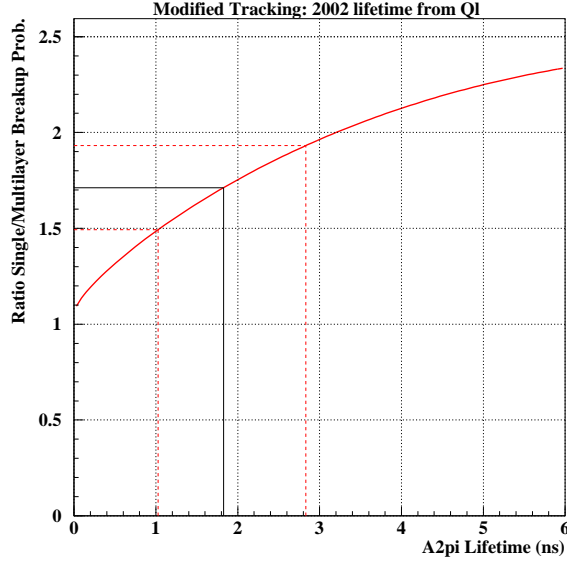


Fig. 6: Breakup probability *ratios*. lifetime parametrization. Breakup and lifetime with corresponding errors for 2002 run with standard tracking in Q_l are shown.

From the goodness-of-fit considerations (Fig. 4), we choose the zero-slope straight line fit (weighted mean) in Fig. 5 to be between 10 and 15 MeV/ c . The averages of the ratios of breakup probabilities are shown in Table 7.

	2002		2003	
Tracking	$\rho(Q_l)$	$\rho(Q)$	$\rho(Q_l)$	$\rho(Q)$
Standard	2.36 ± 0.36	2.93 ± 0.60	1.58 ± 0.24	2.02 ± 0.46
Modified	1.65 ± 0.20	2.18 ± 0.53	1.41 ± 0.23	2.31 ± 0.69

Table 7: Pionium lifetimes as a function of Q_l and Q obtained with the breakup probability ratios method. The values correspond to the breakup probability differences averaged over 10 to 15 MeV/ c intervals.

It can be clearly seen that the breakup probability ratios are prone to large variations in Q_l and Q , with a few values of ρ even lying outside ρ vs. τ dependence (Fig. 6). We can cross-check these results with an MC-generated atomic shape fit found in Fig. 8.8 of Ref. [1] to ensure that the loss accuracy is not caused by poor statistics. The results are shown in Table 8. The ratios

obtained with the atomic shape agree within 1σ with the residuals above and, like the latter, are also seen to vary significantly in Q_l and Q .

	2002		2003	
Tracking	$\rho(Q_l)$	$\rho(Q)$	$\rho(Q_l)$	$\rho(Q)$
Standard	2.01	2.41	1.74	1.83
Modified	1.79	2.18	1.43	1.75

Table 8: Lifetime estimates (shown without statistical errors) from the results of Fig. 8.8 in Ref.[1] and Table 6.

The Effect of the Finite Size Coulomb-Correlation Function

We have also looked into the effects of the finite-size correction to the Coulomb enhancement function $A_c(Q)$, as applied to the breakup probability *difference* method. The parametrization applied to the Q distribution is given by:⁶

$$F_{fs}(Q) = 1.0017 - 0.0285 [(1 + (0.278 \cdot Q)^2)^{-0.421} - 1]. \quad (10)$$

The parametrization in Q_l has been found by numerically integrating the function $A_c(Q)F_{fs}(Q)$.

This function was applied to the *reconstructed* Coulomb pairs produced with modified tracking. The effective K -factor has been assumed to be unchanged. The new background was used to find the breakup probability differences in Q_l and Q for 2002 data in the way analogous to the previous section. for various fit ranges are shown in Fig. 7. A summary of the essential values used to find ΔP_{br} is found in Table 9. The spread in lifetime values is then $1.96_{-0.72}^{+0.85}$ fs for Q_l and $1.61_{-0.74}^{+0.87}$ fs for Q . These results are virtually unchanged from those using the unmodified Coulomb correlation function (see two bottom left entries in Table 5). This contrasts with the results obtained the method of the ratio breakup probabilities, where, using the combined Q_l/Q fit and the atomic shape, 0.31 fs increase in lifetime has been found.

⁶A preliminary version of F_{fs} , with a more pronounced effect on the Coulomb distribution, has been used here. A more up-to-date parametrization may be found in [6].

2002 Modified Tracking (FS correction)		
	Q_l	Q
$\delta_{Q_l, Q}$	1504 ± 438	1315 ± 499
$N_{cc}(Q_l, Q < Q_{cut})$	54660 ± 2844	71934.4 ± 3174.64
ΔP_{br}	0.1638 ± 0.0490	0.1405 ± 0.0543

Table 9: Differentials from Table 1, the integral number of Coulomb pairs modified by the finite-size correction and the resulting values of ΔP_{br} for Q_l and Q averaged over 8 to 15 MeV/c intervals. The values found in this table are to be compared with the corresponding ones of Table 4.

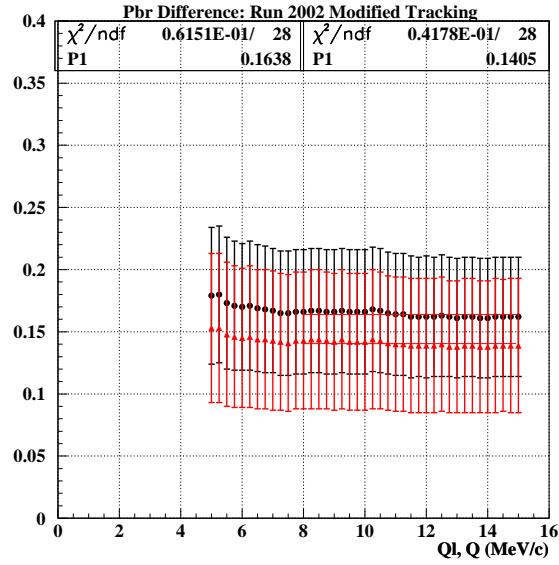


Fig. 7: Breakup probability differences in Q_l and Q as a function of the fit range. The finite-size correction to the Coulomb-correlation function has been applied here.

Comparison of the Methods of Breakup Probability Differences and Ratios

Comparing Tables 5 and 7 we find that the method of breakup probability differences yields a closer agreement in lifetimes in Q_l and Q with standard tracking than with the method of ratios. This closer agreement is attributable to the steeper slope of the ΔP_{br} vs. τ , as compared to the ratio of probabilities ρ vs. τ (Fig. 2 and 6). However, agreement in ΔP_{br} 's and lifetimes in Q_l and Q has not been observed for the *modified* tracking. A sizable disagreement is most clearly in evidence in the subtraction of the experimental Q_l and Q distributions (Tables 5 and 7).

Applying the finite-size correction (assuming an unchanged K_{eff}) leads to the increase of 4 to 5% in the integrated number of the Coulomb pairs (see N_{cc} entries in Table 4 and 9). This corresponds to 4 to 5% decrease in the value of ΔP_{br} . The fact that this decrease in ΔP_{br} is not reflected in the results of Table 9 can be explained by a) the imprecision of fitting of ΔP_{br} with sizable statistical errors and b) by the fact that, as has been found in Ref [7], the effective K -factor decreases slightly, by a few percent (1.7% for 2001 data) due to the finite-size correction. Taking this into account, our 4 to 5% decrease in ΔP_{br} would, in fact, become *smaller*, while the values of ΔP_{br} found in Table 9 would *increase* for the same reason, and the better agreement between the two values would be obtained. With a 1.7% decrease in K_{eff} (we assume that the influence of the finite-size correction on K_{eff} does not change between 2001 and 2002/2003 data) and a 5% increase in N_{cc} , ΔP_{br} would increase by 3.2%. According to the parametrization in Fig. 2 and taking the highest value of the breakup probability (0.196) from Table 9 (this corresponds to the smallest slope in ΔP_{br} vs. τ parametrization), would result in 0.11 fs increase in lifetime. Even assuming, somewhat drastically, the value of ΔP_{br} increase of 4% leads to 0.15 fs increase in τ . The actual increase when the combined Q_l/Q fit is performed would, in fact, be lower. The systematic error due to the finite-size correction represents a clear improvement of the ratios method where a 0.31 fs increase in lifetime has been observed. It should be stressed, however, that a full MC simulation and reconstruction is necessary for a more accurate assessment of the finite-size effect.

Due to the close agreement of the lifetime values from Q_l and Q distributions obtained with the standard tracking (Section 1) and the stability of the

results after applying the finite-size correction (Section 3), we have strong reasons to believe that the method of breakup probability differences offers a good way to analyze the dual-target data.

Acknowledgments

Many ideas for this note came from L. Nemenov and L. Tauscher, whose help I gratefully acknowledge.

References

- [1] D. Goldin, “Measurement of $\pi^+\pi^-$ Bound State Lifetime with the DIRAC Spectrometer at CERN”, Ph.D. Thesis. (<http://cdsweb.cern.ch/search.py?recid=823402&ln=en>).
- [2] P. Zrelov and V. Yazkov, “The GEANT-DIRAC simulation program,” http://zrelov.home.cern.ch/zrelov/dirac/montecarlo/instruction/_instruct26.html.
- [3] D. Drijard, M. Hansroul and V. Yazkov, “The DIRAC Offline User Guide,” <http://dirac.web.cern.ch/DIRAC/Userguide.html>.
- [4] C. Santamarina, M. Schumann, L. G. Afanasyev and T. Heim, “A Monte Carlo Calculation of the Pionium Break-up Probability with Different Sets of Pionium Target Cross Sections,” J. Phys. B. At. Mol. Opt. Phys. **36**, 4273 (2003) [arXiv:physics/0306161].
- [5] R. Lednicky and J. Smolik, Private communication (2003).
- [6] R. Lednicky, “Finite-size effects on two-particle production in continuous and discrete spectrum,” DIRAC Note **04-06**.
- [7] C. Schuetz, “Measurement of the breakup probability in a Nickel target with the DIRAC spectrometer,” Ph.D. Thesis. (<http://cdsweb.cern.ch/search.py?recid=732756&ln=en>)